# Atomistic modeling of thermodynamic properties of Pu-Ga alloys based on the Invar mechanism

Tongsik Lee,* Christopher D. Taylor,† A. C. Lawson, Steven D. Conradson,
Shao Ping Chen, A. Caro, and Steven M. Valone
*Los Alamos National Laboratory, Los Alamos, New Mexico 87545, USA*

Michael I. Baskes
*Department of Aerospace Engineering, Mississippi State University, Mississippi State, Mississippi 39762, USA;*
*Los Alamos National Laboratory, Los Alamos, New Mexico 87545, USA;*
*Department of Mechanical and Aerospace Engineering, University of California, San Diego, La Jolla, California 92093, USA;*
*and Department of Materials Science and Engineering, University of North Texas, Denton, Texas 76207, USA*
(Received 13 September 2013; revised manuscript received 9 May 2014; published 29 May 2014)

We present an atomistic model that accounts for a range of anomalous thermodynamic properties of the fcc $\delta$ phase of Pu-Ga alloys in terms of the Invar mechanism. Two modified embedded atom method potentials are employed to represent competing electronic states in $\delta$-Pu, each of which has an individual configuration dependence as well as distinct interactions with gallium. Using classical Monte Carlo simulations, we compute the temperature dependence of various thermodynamic properties for different dilute gallium concentrations. The model reproduces the observed effects of excessive volume reduction along with a rapid shift in thermal expansion from negative to positive values with increasing gallium concentration. It also predicts progressive stiffening upon dilute-gallium alloying, while the calculated thermal softening is nearly independent of the gallium concentration in agreement with resonant ultrasound spectroscopy measurements in the literature. Analysis of the local structure predicted by the model indicates that the distribution of the gallium atoms is not completely random in the $\delta$ phase due to the presence of short-range order associated with the Invar mechanism. This effect is consistent with the nanoscale heterogeneity in local gallium concentration which is observed in recent extended x-ray absorption fine structure spectroscopy experiments. Implications of the Invar effect for phase stability and physical interpretations of the two states are also discussed.

DOI: 10.1103/PhysRevB.89.174114 PACS number(s): 61.50.Ah, 61.66.Dk, 61.72.S−, 62.20.−x

## I. INTRODUCTION

The unusual properties of plutonium and its alloys have been difficult to understand [1,2]. Among the six equilibrium solid phases of elemental plutonium at atmospheric pressure, the fcc $\delta$ phase possesses a variety of anomalous properties over its narrow stability range of temperature from 593 to 736 K. These include an extraordinarily high elastic anisotropy, the largest atomic volume (albeit the only close-packed structure among the allotropes), negative thermal expansion, and strong thermal softening. While the brittle monoclinic $\alpha$ phase is the most stable state in its unalloyed form at ambient temperature and pressure, the ductile $\delta$ phase can be retained down to room temperature by the addition of relatively small amounts of certain, typically trivalent, elements, such as gallium or aluminum. The $\delta$ phase also exhibits extreme sensitivity to the dilute alloying required for its retention. With increasing gallium concentration, the system undergoes excessive volume reductions while its thermal expansion is driven towards positive values, yet exhibits strong thermal softening virtually independently of the concentration.

These macroscopic anomalies appear to be rather perplexing from the conventional view of solids. Although many suggestions have been put forward to understand the atomistic mechanisms for negative thermal expansion of materials, those that rely solely on large transverse vibrational amplitudes are inadequate to account for the negative thermal expansion of bulk closed-packed structures at high temperatures [3]. Besides, the strong thermal softening indicated in experiments is seemingly contradictory to the negative thermal expansion from the point of view of the standard Debye-Grüneisen theory, in which growing lattice anharmonicity is always associated with positive volume expansion. Moreover, the lattice contraction of $\delta$-Pu by the addition of gallium shows excessive negative deviation from Vegard's law for ideal solutions. As yet, there is no proper understanding of the retention mechanism and concomitant thermoelastic effects that appear upon dilute alloying.

Knowledge of the local structure at the atomic level is essential for obtaining a deeper understanding of the mechanical properties and phase stability of a system. While x-ray diffraction data [4] indicate that the gallium atoms form a substitutional solid solution in $\delta$-Pu, extended x-ray absorption fine structure (EXAFS) spectroscopy studies [5–8] have shown that the local structure around the gallium atoms in dilute alloys is disordered by significant contraction of the Pu-Ga bonds, $\sim$3%–4% shorter than the Pu-Pu bonds in pure $\delta$-Pu. It was found that all twelve of the nearest neighbors of the gallium atoms are plutonium, and the local environment around the gallium atoms is nearly independent of the concentration. Further examination of vibrational properties revealed that

*Current address: Department of Materials Science and Engineering, Massachusetts Institute of Technology, Cambridge, Massachusetts 02139, USA; tongsikl@mit.edu
†Current address: Strategic Research & Innovation, DNV GL, Dublin, Ohio 43017, USA; Fontana Corrosion Center, Department of Materials Science and Engineering, The Ohio State University, Columbus, Ohio 43210, USA.

 

the Pu-Ga bonds are considerably more stable and stiffer than the Pu-Pu bonds [9,10]. Conradson *et al.* [11] recently observed that the gallium atoms in the $\delta$ phase are not randomly distributed, but self-organize to form a quasi-intermetallic of composition $Pu_{25-30}Ga$. Although the gallium atoms appear to avoid direct bonding and repel each other at the nearest-neighbor distance, they act to attract each other by clustering over several nanometers, resulting in nanoscale heterogeneity in local composition.

The local contraction in the Pu-Ga bonds predicted from a density-functional theory (DFT) calculation within the local-density approximation [12] was found to be much weaker than the EXAFS data. Sadigh and Wolfer [13] have subsequently shown in their DFT study in the generalized gradient approximation (GGA) with spin polarization that the excessive reduction of the Pu-Ga bond cannot arise solely from the size misfit and associated elastic strains, but rather that its major contribution comes from the volume reduction of the plutonium atoms surrounding the gallium solute atom induced by electron delocalization. Moore *et al.* [14,15] further discussed that the twelve nearest-neighbor bonds in the $\delta$ phase of unalloyed plutonium are not equivalent, and thereby lead to the reduction of the crystal symmetry into the monoclinic space group and the unusually high elastic anisotropy of this phase. They pointed out that the bond strengths around a gallium atom in dilute-gallium alloys become less anisotropic, and this mechanism is responsible for the retention of the fcc structure. Furthermore, by employing the cluster variation method, Robert *et al.* [16,17] demonstrated that chemical short-range order in the $\delta$-solid solution can have a strong influence on the stability of this phase in the Pu-Ga phase diagram.

An analogy to the Invar alloys has shed light on the understanding of the characteristic temperature variations of the thermodynamic properties of $\delta$-Pu and its alloys. Eriksson *et al.* [18] described in their mixed-level model that the transition from itinerant to localized electronic behavior in the actinide series takes place progressively within plutonium, and that multiple electronic configurations with varying degrees of delocalization of distinct equilibrium volumes exist close in energy for the $\delta$ phase. They anticipated that the unusual thermal properties in $\delta$-Pu result from the competing electronic states in the fcc structure in a manner analogous to the Invar alloys. Lawson *et al.* [19,20] indeed modeled the temperature variation of the thermodynamic properties of the $\delta$ phase of plutonium alloys by means of the two-state model of Weiss [21], which was originally developed to explain the anomalous properties of the iron-based Invar alloys. The model postulates that the plutonium atoms in the fcc structure can exist in two electronic configurations closely spaced in energy, and describes the entropy associated with the thermal excitations between those two states in terms of a Schottky two-level statistical-mechanical treatment.

The recognition of the importance of the Invar effect in $\delta$-Pu has led to the development of an atomistic model utilizing effective interatomic potentials that accounts for the negative thermal expansion in its unalloyed form [22]. The Invar mechanism is built into the model in such a way that the plutonium atoms in the fcc structure are effectively characterized by two binding energies corresponding to differing electronic states individually coupled to the atomic configuration with respective equilibrium volumes. Employing two modified embedded atom method (MEAM) potentials to represent these two electronic states, the model incorporates thermal excitation between these states using the classical Monte Carlo (MC) method. The model provides an atomic-scale description of how the thermal expansion is suppressed as the plutonium atoms are excited to the small-volume state at elevated temperature, and the excess entropy associated with this excitation concurrently gives rise to a Schottky-like anomaly in the heat capacity.

Due to the difficulties involved in its strong electron correlations, there is no established first-principles method capable of making reliable predictions of the electronic structure of plutonium, even for the ground state of its elemental form, let alone the complex effects introduced by temperature and chemical alloying. Hence, an atomistic approach is a practically feasible microscopic alternative to address these problems. In this study, we extend the application of the two-state MEAM model developed for unalloyed $\delta$-Pu in Ref. [22] to the modeling of $\delta$ Pu-Ga alloys. The goal of this study is to present an atomistic model that reproduces a variety of characteristic thermodynamic properties of these alloys in a consistent manner. The atomistic model developed in this study is conceptually based on the earlier analyses in terms of the noninteracting Weiss model [19,20]. We demonstrate how the introduction of atomic interactions, constructed upon simple mechanisms in energetics, can give rise to a detailed microscopic description of the temperature and dilute-alloying effects in this system.

The reminder of this paper is structured as follows. In Sec. II, the computational methods and some details of the model potentials are outlined. We then validate in Sec. III the performance of the present model by computing various response properties as a function of temperature and gallium concentration, in close reference to experimental data available in the literature. We further address the connection of those properties with the energy-volume relationships, followed by an investigation of the local structure. Some remarks and discussion concerning phase stability and physical interpretations of the present atomistic model are provided in Sec. IV. Finally, conclusions are given in Sec. V.

## II. SIMULATION METHODS

### A. Monte Carlo method

While the original Weiss model relies on the ideal Schottky two-level system, its underlying concept has been adopted to atomistic modeling with interatomic potentials for the Invar iron alloys [23,24], manganese alloys [25], and elemental $\delta$-Pu [22]. In the two-state description, we assume that the atoms in a certain crystal can exist in two nearly degenerate yet distinct electronic or magnetic states, hereafter referred to as states 1 and 2 for simplicity. The system in this description is similar to a binary alloy if we interpret the atoms in each state as having distinguishable "chemical identity" or "type," in accord with the notion of *self-intermetallic* [26]. In this case however, the state of each atom can fluctuate under the influence of thermal agitation, pressure, or chemical alloying. The number of atoms in each state, $N_1$ and $N_2$, is thereby not held fixed but varies, while the total number of atoms $N$ is conserved. We wish to

find the equilibrium volume and fraction of the atoms in each state at a constant external pressure $p$ and temperature $T$. It is pertinent to implement atomistic MC simulations in the semi-grand ensemble [27,28] at constant $p$ and $T$, setting the relative chemical potential between the two states, $\Delta\mu$, to zero [22].

Let us denote by $\{l\}$ the configuration of states of $N$ atoms $\{l_1,l_2,\ldots,l_N\}$ at a configuration of atomic positions $\{\mathbf{r}\}=\{\mathbf{r}_1,\mathbf{r}_2,\ldots,\mathbf{r}_N\}$. Each component of $\{l\}$ takes on either state 1 or 2, independently of the spatial configuration $\{\mathbf{r}\}$. Suppose now that the $i$th atom alters its state from $l_i$ to $l_i'$ $(\neq l_i)$ at temperature $T$. We describe this type of thermal excitation in terms the Schottky statistics by performing a trial move according to the Metropolis acceptance rule (at $\Delta\mu=0$)

$$\mathrm{acc}(l_i\rightarrow l_i')=\min\left\{1,\frac{g_{l_i'}}{g_{l_i}}\exp(-\beta[U(\{l_i'\})-U(\{l_i\})])\right\}, \quad (1)$$

where $\beta=(k_{\mathrm{B}}T)^{-1}$ with the Boltzmann constant $k_{\mathrm{B}}$, $g_l$ is the degeneracy factor of state $l$, $\{l_i\}$ indicates the $\{l\}$ for which the $i$th atom is in state $l_i$ at a given $\{\mathbf{r}\}$, and $U$ is the potential energy per cell including the interactions among the atoms in image cells. The above type of trial moves taking place in the state space $\{l\}$ are implemented in conjunction with conventional trial moves in the coordinate space $\{\mathbf{r}\}$. The latter moves are in practice sampled individually in the scaled coordinates $\{\mathbf{s}\}=\{\mathbf{s}_1,\mathbf{s}_2,\ldots,\mathbf{s}_N\}$ and the volume scale $V$ of the periodic cell, where $\mathbf{r}_i=V^{1/3}\mathbf{s}_i$, as though those degrees of freedom are independent of each other [29].

We further employ the method of parallel tempering [28,30,31] in order to enhance the sampling efficiency. This method is implemented by simulating $M$ replicas of the constant-$\Delta\mu pT_k$ ensembles ($k=1$–$M$), each of which differs in temperature $T_k$, and including another type of Metropolis trial move that swaps the configurations belonging to two replica ensembles at adjacent temperatures. Let us denote by $\{k\}$ the configuration $(\{\mathbf{r}\},\{l\})$ that originally belongs to the $k$th ensemble. The Metropolis acceptance rule for a trial move exchanging the configurations of the $k$th and $k'$th ensembles (at $p=0$ and $\Delta\mu=0$) is given by

$$\begin{aligned}&\mathrm{acc}((\{k\},\beta_k),(\{k'\},\beta_{k'})\rightarrow(\{k'\},\beta_k),(\{k\},\beta_{k'}))\\&\quad=\min\{1,\exp\{(\beta_k-\beta_{k'})[U(\{k\})-U(\{k'\})]\}\},\end{aligned} \quad (2)$$

where $\beta_k=(k_{\mathrm{B}}T_k)^{-1}$.

Various response functions can be conveniently obtained from mean-square fluctuations of state variables [32]. The properties of interest are the isobaric heat capacity $C_p$, the coefficient of thermal expansion $\alpha$, and the isothermal compressibility $\kappa_T$, all of which are directly comparable with experimental data. These quantities are first derivatives of the state variables, and are related to the complete set of second derivatives of the Gibbs free energy $G$, such that

$$-\frac{C_p}{T}=-\left(\frac{\partial S}{\partial T}\right)_p=\frac{\partial^2 G}{\partial T^2}, \quad (3)$$

$$V\alpha=\left(\frac{\partial V}{\partial T}\right)_p=\frac{\partial^2 G}{\partial T\partial p}, \quad (4)$$

$$-V\kappa_T=\left(\frac{\partial V}{\partial p}\right)_T=\frac{\partial^2 G}{\partial p^2}, \quad (5)$$

where $S$ is the entropy of the system. The above expressions can be rewritten in terms of the fluctuations in potential energy and volume, and their joint fluctuations, as

$$C_p/k_{\mathrm{B}}=(3N+1)/2+\beta^2\langle(U-\langle U\rangle)^2\rangle, \quad (6)$$

$$\langle V\rangle\alpha=k_{\mathrm{B}}\beta^2\langle(U-\langle U\rangle)(V-\langle V\rangle)\rangle, \quad (7)$$

$$\langle V\rangle\kappa_T=\beta\langle(V-\langle V\rangle)^2\rangle, \quad (8)$$

at $p=0$, where the brackets indicate averages over the constant-$\Delta\mu pT$ ensemble. The above formulas furnish an efficient method for systematic analysis of these thermodynamic properties on a coherent basis.

### B. Details of model potentials

As remarked earlier, accurate calculations of the electronic structures of actinide materials have been hampered by the challenge associated with a proper treatment of their strong electron correlations, which cannot easily be described within the DFT framework based on the traditional one-electron band-structure approach. Although several innovative proposals have been advanced to capture the elusive electronic nature of plutonium (e.g., Refs. [33,34] and references therein), such as DFT implemented with onsite-Coulomb corrections or dynamical mean-field theory, there is as yet no first-principles method that offers a reliable database of the ground-state properties of this system. In addition, there has been no direct observational evidence, as of now, for the existence of the small-volume state in $\delta$-Pu postulated in our two-state description. As a result, there is a paucity of first-principles information and experimental data pertaining to physical properties which can be utilized to make an unambiguous determination of the interatomic potentials for each element and their cross interactions in the present model. Hence, in this study we opt to determine the free parameters in the model so as to reproduce known measured thermodynamic properties, such as volume and thermal expansion, with respect to temperature and gallium concentration, as described below in detail.

Plutonium is a highly covalent material due to the strong directionality of the $f$-electron orbitals, and therefore we employ the MEAM potential [35] as an interatomic-potential model to incorporate the angular dependence of electron densities. The parameters for the MEAM potentials used in this study are given in Tables I(a) and I(b). For simplicity, the state 1 and the state 2 of plutonium in the $\delta$ phase are henceforth referred to as "Pu1" and "Pu2," respectively. The type of interactions for each parameter is specified by its indices; Pu1, Pu2, and gallium are represented in each index by 1, 2, and 3, respectively. The parameters have been modified from previous works [22,36–40]. Details of the MEAM formalism are described in the cited literature.

We adopt for Pu1 the MEAM parameters originally provided in Ref. [36], but with two modifications: $t_1^{(3)}=0$ and $\delta_{1,1}=0$. The finite value of $t_1^{(3)}$ is generally correlated with the inversion symmetry of a crystal, and its original negative value (–0.8) was given to destabilize the $\delta$ phase over the monoclinic $\alpha$ phase at low temperatures. Setting $t_1^{(3)}$ to zero ensures that Pu1 is at least metastable in the fcc structure even at low temperatures, though only weakly because of the small

TABLE I(a). MEAM parameters suggested in this work. $k$ and $k'$: indices specifying the type of interaction; $E^{c}$: cohesive energy (in eV); $r^{e}$: equilibrium nearest-neighbor distance (in Å); $\alpha$: exponential-decay factor for the universal energy function; $\delta$: short-range correction factor; $A$: scaling factor for the embedding energy; $\beta^{(l)}$ ($l = 0$–3): exponential-decay factor for the atomic densities; $t^{(l)}$ ($l = 0$–3): weighting factors for the atomic densities; $\rho^{0}$: density-scaling factor.

| | $k,k'$ | $E^{c}_{k,k'}$ | $r^{e}_{k,k'}$ | $\alpha_{k,k'}$ | $\delta_{k,k'}$ | $A_k$ | $\beta^{(0)}_k$ | $\beta^{(1)}_k$ | $\beta^{(2)}_k$ | $\beta^{(3)}_k$ | $t^{(1)}_k$ | $t^{(2)}_k$ | $t^{(3)}_k$ | $\rho^{0}_k$ |
|---|---|---|---|---|---|---|---|---|---|---|---|---|---|---|
| Pu1 | 1,1 | 3.800 | 3.281 | 3.310 | 0.000 | 1.05 | 2.39 | 1.00 | 6.00 | 9.00 | 1.00 | 4.14 | 0.00 | 1.0 |
| Pu2 | 2,2 | 3.680 | 3.253 | 3.928 | 0.000 | 1.05 | 2.39 | 1.00 | 6.00 | 9.00 | 1.00 | 0.50 | 0.00 | 1.0 |
| Ga | 3,3 | 2.897 | 3.003 | 4.420 | 0.097 | 0.97 | 4.80 | 3.10 | 6.00 | 0.50 | 2.72 | 2.06 | −4.00 | 0.7 |
| Pu1-Pu2 | 1,2 | 3.765 | 3.267 | 3.465 | 0.000 | | | | | | | | | |
| Pu1-Ga | 1,3 | 3.499 | 3.215 | 4.143 | 0.300 | | | | | | | | | |
| Pu2-Ga | 2,3 | 3.964 | 3.187 | 6.675 | 0.500 | | | | | | | | | |

TABLE I(b). Angular screening parameters for the MEAM potentials. "Pu" stands for either Pu1 or Pu2.

| | Pu-Pu-Pu | Pu-Ga-Pu | Pu-Pu-Ga | Pu-Ga-Ga | Ga-Pu-Ga | Ga-Ga-Ga |
|---|---|---|---|---|---|---|
| $C_{\max}$ | 2.8 | 2.8 | 2.8 | 2.8 | 2.8 | 2.8 |
| $C_{\min}$ | 2.0 | 1.4 | 2.0 | 1.4 | 1.4 | 1.4 |

value of its shear elastic constant $C'$ (∼5 GPa). In this work, we do not directly address the relative stability among phases, but only briefly allude to its relation to the Invar mechanism in Sec. IV. The null value of $t^{(3)}_1$ also eliminates the contribution from the third-partial electron density. We do not speculate in this study on its direct association with the *f*-electron density (cf. Ref. [41]). Fitted values of elastic constants in the fcc structure remain intact upon this modification, so that the Pu1 potential still reproduces the correct elastic anisotropy, $A \equiv C_{44}/C' \sim 6.7$ at 0 K, which is in close agreement with experiment (∼7.1 [42]). The original value of $\delta_{1,1}$ (0.46) in Ref. [36] was determined from the experimental pressure derivative of the bulk modulus of the $\alpha$ phase. We do not adopt this value in the present analysis of the $\delta$ phase, as we are not concerned with the $\alpha$ phase.

In the two-state description of the Invar mechanism, Pu2 is assumed to be higher in energy by $\Delta E$ but lower in volume by $\Delta V$ than Pu1 in equilibrium. The magnitude of $\Delta E$ is comparable to the thermal energy. We adopt the value of $\Delta E = 0.12$ eV (∼1400 K) from the previous analyses based on the Weiss model conducted in Refs. [19,20]. In the original Weiss model, it is only the $\Delta E$ that controls the thermal accessibility between the two states. In the present atomistic description, in contrast, the accessibility depends upon the details of the interatomic potentials.

We determine the value of $\Delta V$ in conformity with a DFT analysis previously conducted by Sadigh and Wolfer [13], according to which the plutonium atoms surrounding a gallium impurity atom in the $\delta$ phase undergo a volume reduction due to electron delocalization. The core idea underlying the present atomistic model is to identify these plutonium atoms of a reduced volume with the Pu2 state, in line with the mechanism conjectured by Lawson *et al.* [20]. In this way, the crystal structure of impurity-stabilized $\delta$-Pu can have a structure similar to that of temperature-stabilized $\delta$-Pu, as hinted by x-ray diffraction measurements [4]. The Pu2-Pu2 bond length is made only marginally shorter than the Pu1-Pu1 bond length by 0.85%, in close agreement with the prediction made in Ref. [13] (0.7%). This choice results in $\Delta V = 0.63$ Å$^3$. Note that this value is considerably smaller than the value selected in the previous study [22], which was taken to be the volume difference between the $\delta$ and $\alpha$ phases (∼4.96 Å$^3$). In this study, we do not assume a direct connection between the Pu2 state and the electronic ground state of $\alpha$-Pu. Although there are a number of combinations among free parameters that would fit the temperature variation of the volume of unalloyed $\delta$-Pu, we attempt to reproduce the gallium-concentration dependence of thermodynamic properties in a cooperative manner with a smaller value of $\Delta V$ than in the previous study.

Relative stiffness between the Pu1 and Pu2 states is another parameter that has a major influence on the thermal accessibility between these states. A previous electronic-structure analysis of $\delta$-Pu within the GGA+$U$ framework [43] has shown that a state with less localized electrons is generally characterized by a larger bulk modulus than a state with localized electrons. In the present model, Pu2 is made stiffer than Pu1 by approximately 40%, according to the interpretation of the two electronic states given above. This value of the relative stiffness was empirically chosen to optimize the thermal accessibility between the two states for the values of $\Delta E$ and $\Delta V$ stated above, such that the negative thermal expansion of unalloyed $\delta$-Pu is correctly reproduced in its stability range at high temperatures. In addition, we made Pu2 less elastically anisotropic ($A \sim 2.3$) than Pu1 as much as possible, such that the former is relatively more stable in the fcc structure than the latter, qualitatively in line with the discussions in Refs. [14,15]. The other MEAM parameters for Pu2 that are uncorrelated with the aforementioned properties are assumed to be identical to those for Pu1.

To obtain the unlike-pair potential between Pu1 and Pu2 atoms, we define the cohesive energy $E^{c}_{1,2}$ of a hypothetical $L1_2$ reference structure of the $Pu1_3Pu2$ alloy as

$$E^{c}_{1,2} = \frac{3E^{c}_{1,1} + E^{c}_{2,2}}{4} - \Delta_{1,2}, \tag{9}$$

where $E^{c}_{1,1}$ and $E^{c}_{2,2}$ are the cohesive energies of Pu1 and Pu2, respectively, and $\Delta_{1,2}$ is the mixing energy between these two components. Our preliminary study [22] demonstrated that the onset temperature at which the average Pu2 occupancy becomes substantial depends sensitively on the balance between the values of $\Delta E$ and $\Delta_{1,2}$, which in turn governs the temperature profile of thermodynamic properties. As described above, the value of $\Delta E$ in this study is adopted from the previous analysis based on the noninteracting Weiss model [19,20], and this choice is largely correlated with the relatively small value of $\Delta_{1,2}$ (=+5 meV) in the present model. We note that this small but positive mixing energy appears to give rise to anomalies in thermodynamic properties at low temperatures around 200 K, well below the eutectoid point on the experimental Pu-Ga phase diagram (at 373 K, below which the $\delta$ phase is no longer the equilibrium phase but separates into the mixture of $\alpha$-Pu and $Pu_3Ga$ [44]). As a simplistic convention, the lattice parameter of the reference structure is determined by a geometric mean, and the exponential-decay factor for the universal binding-energy function is defined by a composition-weighted average similar to the first term on the right-hand side of Eq. (9).

The ratio between the degeneracy factors of the Pu1 and Pu2 states also impacts the thermal accessibility between these states. Owing to the current lack of detailed information of the electronic structure of $\delta$-Pu, a nominal value of $g_1/g_2 = 1$ is taken in this study, as in the previous analysis in terms of the Weiss model [19]. This choice would not be too far off from its actual value, however. Our simulations indicate that the system cannot generate a sufficient number of Pu2 atoms to drive the negative thermal expansion at high temperatures in unalloyed $\delta$-Pu when $g_1/g_2$ is much greater than unity, while it tends to undergo an undesired, discontinuous isostructural transition when $g_1/g_2$ is much less than unity, being qualitatively similar to the observation previously made in the analysis of a two-level interacting model [45].

The parameters for gallium are taken directly from Ref. [46]. The cross-pair potentials for the Pu1-Ga and Pu2-Ga interactions are constructed at the $L1_2$ reference structures of the $Pu1_3Ga$ and $Pu2_3Ga$ alloys, respectively. The cohesive energies of these compounds, $E^{c}_{1,3}$ and $E^{c}_{2,3}$, are defined in a fashion similar to Eq. (9), in terms of the cohesive energies of individual components and the mixing energies between these components. We attempt to characterize these interactions on the basis of the aforementioned mechanism of Lawson *et al.* [20] and the GGA analysis of Ref. [13]. This mechanism ensures that, in the fcc structure, gallium impurities induce electron delocalization in their neighboring plutonium atoms, so as to transition to the electronic states of these plutonium atoms from Pu1 to Pu2, so that Pu2-Ga bonds are energetically preferred to Pu1-Ga bonds. Gallium atoms are subsidiarily assumed to be immiscible in the Pu1 fcc crystal, so that the $Pu1_3Ga$ compound is neither stable in the $L1_2$ reference structure nor in solid solution. The values of $r^{e}_{1,3}$, $\Delta_{1,3}$, and $\alpha_{1,3}$ are determined from the atomic volume, formation energy, and bulk modulus of the random fcc-solid solution of the same composition (25 at.% gallium) obtained from the density-functional calculations in Ref. [47]. The value of $\delta_{1,3}$ is found to have only a minor effect on thermal expansion of dilute-gallium alloys in the present model. Hence we maintain its original value for the Pu-Ga interaction from Ref. [37].

Experimentally the $Pu_3Ga$ alloy forms a stable $L1_2$ compound [4]. For simplicity, we neglect the subtlety associated with the tetragonal distortion of this compound in its low-temperature phase. Given that the plutonium atoms always have gallium first-nearest neighbors in this structure, the plutonium atoms in this compound are considered to all be in the Pu2 state at 0 K, according to the mechanism mentioned above. Hence, we adopt for the Pu2-Ga interaction in the present model the parameters for the Pu-Ga interaction previously given in Ref. [37] which were fitted to the experimental data of the $L1_2$ $Pu_3Ga$ compound. In response to $E^{c}_{2,2}$ being smaller than $E^{c}_{1,1}$, the latter of which was originally viewed in Ref. [37] as the cohesive energy of plutonium in the stable $L1_2$ $Pu_3Ga$ compound, the value of $\alpha_{2,3}$ in the present model is marginally modified so as to reproduce the same bulk modulus as that in the reference. The value of $\delta_{2,3}$ has been slightly increased from the original value from Ref. [37], such that the experimental thermal expansion of the 2 at.%–gallium alloy is reproduced. We confirmed that the $L1_2$ phase of the $Pu2_3Ga$ alloy is stable up to 800–900 K, above which the long-range order disappears, while the short-range order remains relatively high.

In defining the average electron density from the partial electron densities [35], the square-root functional form is adopted for all types of interactions. Pair potentials and electron densities are smoothly truncated by the angular screening procedure to limit the range of interactions [48]. The angular screening parameters are taken from Ref. [37] and are shown in Table I(b). We assume that the Pu1 and Pu2 atoms do not differ in their angular screening behavior. The cutoff radius and the cutoff region are taken to be 5.0 Å and 0.5 Å, respectively.

At this point, we wish to highlight two important features of the model energetics described above. First, in the fcc structure, the Pu2 state is energetically higher but lower in volume in equilibrium than the Pu1 state. The energy separation between these states is within the thermal energy range. Second, the Pu2-Ga bond is substantially stronger, shorter, and stiffer than the Pu1-Ga bond, conforming with the EXAFS analyses provided in Refs. [9,10]. The former is responsible for the anomalous effects of the thermal properties of $\delta$-Pu, and the latter plays an essential role in the drastic change of these properties in response to dilute-gallium alloying, as will be discussed in detail in Sec. III.

### C. Computational details

We demonstrate the performance of the atomistic model described above by computing various equilibrium properties as a function of temperature. Classical MC simulations are conducted in parallel using $M = 64$ replicas of a semigrand ensemble all with $\Delta\mu = 0$ and $p = 0$. Each of replica differs in temperature, ranging from $T_{\min}$ =250 K to $T_{\max}$ =1000 K. Temperature $T_k$ at the $k$th replica ($1 < k \leqslant M$) is determined according to a geometric progression defined by

$$T_k = (T_{\min}/T_{\max})^{(1-k)/(M-1)} T_{\min}, \tag{10}$$

in order to optimize the acceptance ratios for parallel tempering at all temperatures [49]. A periodic cell containing $N = 500$

atoms is simulated at each temperature under the dynamic boundary conditions. All simulation cells initially are a perfect fcc crystal with the lattice parameter of experimental $\delta$-Pu, and all the plutonium atoms are in the Pu1 state. The variation of dilute-alloying effects is examined for four values of gallium concentration: 0, 2, 4, and 6 at.%.

The sampling strategy taken in this study is similar to that in Refs. [22,50]. Within each replica ensemble, the following four types of configuration changes are made: (i) a random displacement in the scaled coordinates of an arbitrarily selected atom, (ii) a random change in the volume scale of the periodic cell, (iii) an identity switch between the Pu1 and Pu2 states for a randomly selected plutonium atom, and (iv) an exchange in position between gallium and either Pu1 or Pu2 atoms in cases for which the gallium concentration is finite. The last type of move is essential to account for the mixing entropy associated with the interdiffusion process in the Pu-Ga alloys. One of the above four types of trials is randomly attempted at each MC move according to certain probability ratios, which are empirically selected to optimize the convergence rate. The choice of the ratios affects the speed of convergence, but the results are independent of the particular choices, provided that simulations are sufficiently converged.

In addition, we perform parallel tempering with a fixed schedule of every 100 moves, where atomic configurations are exchanged between adjacent replicas at both lower and higher temperatures in succession [51]. Uncorrelated sequences of random numbers are generated simultaneously at these replica ensembles by utilizing the scalable parallel random number generator [52]. We note that in the present MC scheme, parallel tempering is a vital sampling technique at low or moderate temperatures, since the acceptance rates for the last two kinds of the aforementioned trial moves are considerably low because of insignificant lattice vibrations.

Statistical averages are obtained with the block averaging method, where each block consists of a half million trial moves. Data were collected from 100 blocks following the discarding of the first few blocks. Quoted statistical errors in the figures presented below indicate one standard deviation, but the error bars are smaller than the symbol size of the data in most cases.

## III. SIMULATION RESULTS

### A. Relative occupation of Pu2 state

Figure 1 shows the temperature dependence of the relative occupation of Pu2 atoms, $N_2/N$, for the four selected gallium concentrations. Here, $N = N_1 + N_2 + N_3$, and the number of gallium atoms $N_3$ is fixed for a given gallium concentration. The temperature profile of the Pu2 occupancy is similar to that obtained from the simple Schottky statistics in the Weiss model, but the curves calculated from the present model exhibit more complicated dependencies on the details of the interatomic potentials which are absent in the Weiss model [22]. For bulk unalloyed $\delta$-Pu, virtually all plutonium atoms remain in the Pu1 state at low temperatures, while they can be excited to the Pu2 state only by thermal agitation (at zero external pressure). The Pu2 atoms come into the system even at 0 K in the presence of gallium impurity atoms, each

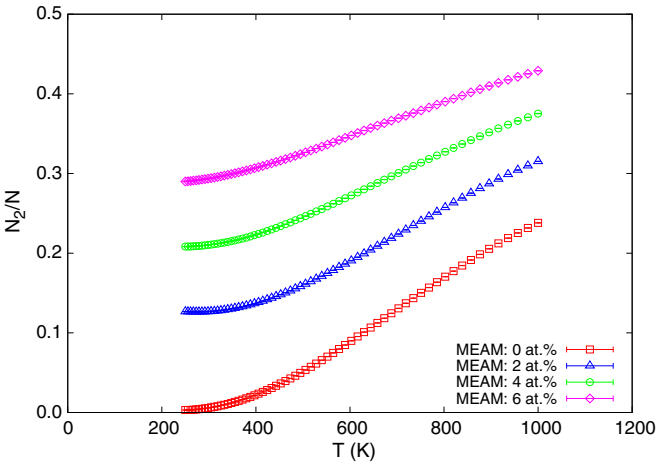


FIG. 1. (Color online) Calculated temperature dependence of the relative occupation of Pu2 atoms for varying gallium concentration.

of which energetically promotes the states of its neighboring plutonium atoms from Pu1 to Pu2.

A particular significance in this setting lies in the fact that the gallium atoms tend to share neighboring Pu2 atoms with other gallium atoms, forming a domain consisting of Pu2 and gallium atoms, which is separated from the other domain of Pu1 atoms in the simulation cell. As a result, the Pu2 occupancy for a given gallium concentration at low temperatures is about a half or less than what is expected from naively conceiving that the gallium atoms, surrounded by twelve first-nearest neighbor Pu2 atoms, are well isolated from each other. As will be discussed in Sec. III F in more detail (and as was previously suggested, in essence, in Ref. [40]), the presence of short-range order in the gallium local structure is closely related to the nanoscale heterogeneity in the $\delta$ phase observed in EXAFS experiments [11].

The temperature variation of the Pu2 occupancies for finite gallium concentrations resembles that for zero gallium concentration, because the Pu2 atoms arise in the Pu1 domain at finite temperature in a similar fashion to the case of unalloyed $\delta$-Pu. A curve for greater gallium concentration, however, shows progressively weaker temperature dependence, as the Pu1 domain is smaller in the system. As will become increasingly evident below, the profile of the Pu2 occupancy observed above is the key to understanding the characteristic variation of the thermodynamic properties of the Pu-Ga alloys with respect to temperature and gallium concentration.

### B. Heat capacity

Shown in Fig. 2 is the calculated isobaric heat capacity $C_p$ per atom (scaled by $k_B$, thus dimensionless) plotted as a function of temperature for the four gallium concentrations. The experimental data measured with adiabatic calorimetry for unalloyed $\delta$-Pu from Ref. [53] and for 3.3 at.% gallium from Ref. [54] are also included in the figure for reference. We note that there also exist previous high-temperature heat capacity data measured with adiabatic calorimetry [55] as well as data obtained indirectly from enthalpy measurements using drop calorimetry [56,57]. These data do not appear to agree well

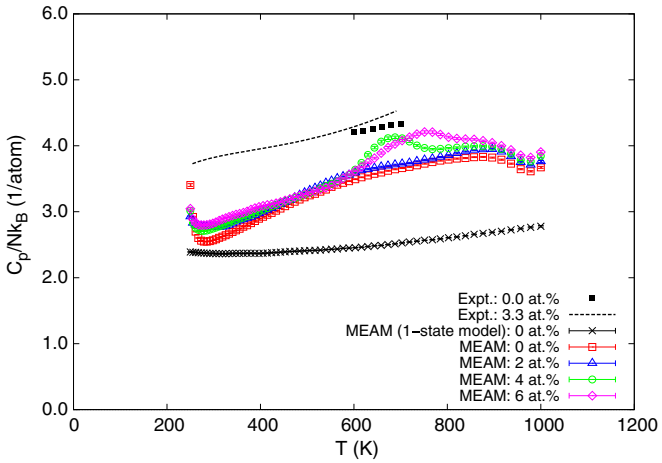


FIG. 2. (Color online) Calculated temperature dependence of the heat capacity per atom, scaled with the Boltzmann constant, for varying gallium concentration. The experimental data from Refs. [53,54] for unalloyed $\delta$-Pu and 3.3 at.%–gallium alloys, respectively, are also included for reference.

with those from Refs. [53,54], the latter of which considered more reliable. Figure 2 also includes the heat capacity data in the case of 0 at.% gallium calculated with a conventional simulation with only Pu1 atoms, i.e., without the two-state mechanism (labeled as "1-state model" in the figure). The same data obtained from a simulation with the two-state mechanism exhibit a marked increment amounting to $1.19Nk_B$ at its peak. This heat capacity increment manifests the excess entropy contribution from the thermal excitation between the two states, similarly to the Schottky anomaly in the Weiss model. The magnitude of the heat capacity increment obtained from the present model is comparable to the value estimated from experiment for pure $\delta$-Pu in Ref. [53] [$\sim$(1.18–1.30)$R$ at 600–700 K, where $R$ is the gas constant].

In the original Weiss model, the temperature variation of the excess heat capacity is directly related to the occupancy of the higher energy state, and the temperature at which a Schottky peak arises depends solely on the magnitude of $\Delta E$ for a given value of the degeneracy ratio. The peak in the Weiss model occurs around the inflection point in the occupation number, which is approximately 0.4 times $\Delta E/k_B$ in the case of $g_1 = g_2$ [58]. The heat capacity data obtained from the present model also indicate close correlation with the relative Pu2 occupation data in Fig. 1, but the position of the anomalous peak depends on the details of the interatomic potentials, and it is located at a much higher temperature in this parametrization than what is predicted by the Weiss model.

The calculated heat capacity data in Fig. 2 show an increasing trend with growing gallium content. Considering that it is the thermal excitation between the two plutonium states that generates excess entropy, one might well anticipate that a system with lower gallium concentration, which includes more Pu1 atoms at low temperatures, would yield a higher heat capacity peak. It is important to note however that in the present model, the above effect is overridden by the contribution from the mixing entropy associated with the interdiffusion between gallium and plutonium, which is enhanced with increasing gallium concentration. We indeed observed that simulations performed with fixed positions of gallium atoms display a reverse trend, i.e., a decreasing heat capacity peak with increasing gallium concentration. The balance between these opposing effects is rather subtle, however, and the heat capacity profile also depends sensitively on fine details of the atomic interactions. Given the scatter of the data available in the scarce experimental literature, it is difficult to establish a definitive trend regarding gallium concentration, but the calculated heat capacity data are qualitatively consistent with the adiabatic calorimetry measurements in Refs. [53,54].

There are at least two apparent reasons for the calculated heat capacity being lower than the experimental data at all temperatures. First, the temperature profile of the heat capacity data obtained from the original MEAM potential for plutonium adopted from Ref. [36] (i.e., the Pu1 state in the present model) shows a mildly concave downward curve (as seen in the data referred to as "1-state model"), leading to substantial reduction from the classical value, $\sim 3Nk_B$. This effect results in the overall reduction of the calculated heat capacity, rendering it lower than experimental data at all temperatures, even when it is incremented by the Invar contribution. Such an effect of reduction in the heat capacity however is not an intrinsic nature of the MEAM potential but most likely is a mere artifact in this particular parametrization of the potential. Second, although the present model accounts for the contribution of the mixing between the two electronic states, none of these states described by the MEAM potential incorporates any effect of electronic thermal excitation, just like any other conventional interatomic-potential model. Experimentally the electronic contribution to the heat capacity was found to be substantial in $\delta$-Pu already at cryogenic temperature [59,60]. Classical simulations are incapable of capturing these electronic effects.

### C. Atomic volume and thermal expansion

The temperature dependence of the calculated atomic volume $V_a$ and the linear coefficient of thermal expansion $\alpha/3$ are respectively shown in Figs. 3 and 4 for the four gallium concentrations. The calculated data of atomic volume are directly compared with neutron diffraction data from Ref. [19] for the same gallium concentrations [61]. These experimental volume data are too sparse to allow us to directly evaluate the experimental thermal expansion coefficient. Instead, for the purpose of reference, we include in Fig. 4 the thermal expansion data obtained by differentiating the fit to the experimental-volume data that is made by means of the Weiss model. (It should be borne in mind that, due to the sparse data points for the experimental volume, the details of these curves are sensitive to the model, and so subject to relatively high uncertainty. Thus, the comparisons are only meant to be qualitative.) The present model reproduces the variation in the atomic volume with respect to both temperature and gallium concentration observed in experiments. Figure 3 shows that the calculated atomic volume undergoes excessive reductions at low temperatures upon gallium addition in close agreement with the experimental data. At the same time, the calculated thermal expansion coefficient displays a gradual shift from negative to positive values with increasing gallium content similarly to the reference data (Fig. 4). The

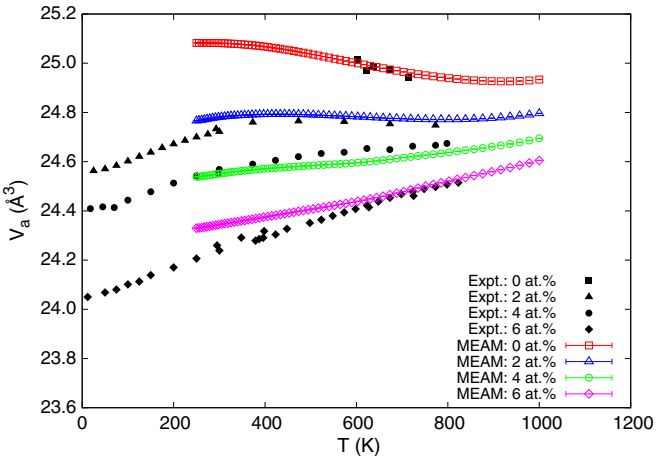


FIG. 3. (Color online) Calculated temperature dependence of the atomic volume for varying gallium concentration. The experimental data from Ref. [19] are also included for comparison.

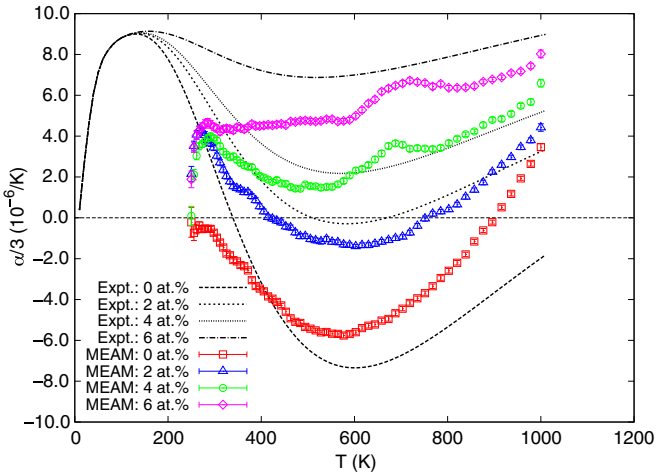


FIG. 4. (Color online) Calculated temperature dependence of the linear coefficient of thermal expansion for varying gallium concentration. The curves obtained by differentiating the fit to the experimental volume data using the Weiss model are also included for reference. Note that these reference curves are subject to relatively high uncertainty due to the sparse data points for the experimental volume.

transition from negative to positive values in the calculated thermal expansion coefficient takes place between 2 and 4 at.%, in accordance with the reference curves as well as the experimental observation made in Ref. [62] (at approximately 3 at.% gallium around 600 K). Notice that each of these effects occurs in concert with the significant gain in the number of Pu2 atoms at low temperatures and its gradual saturation at high temperatures with increasing gallium concentration, indicated in Fig. 1.

The calculated atomic volume data appear to be rather higher than the experimental data at low temperatures. One plausible explanation for the apparent discrepancy could be based upon the two-state mechanism. The calculated data from the present MC simulations represent the equilibrium at all temperatures, provided that the simulations are well converged. The periodic cell used in these simulations is not sufficiently large to account for phase decomposition, but the system is constrained to simulate the $\delta$ phase at low temperatures. The experimental measurements below the eutectoid temperature of 373 K, on the other hand, must have been made on metastable samples of $\delta$ Pu-Ga alloys, quenched from a certain higher temperature at which the $\delta$ phase is the most stable state. Below the eutectoid point, these quenched samples should contain greater amounts of Pu2 atoms with lower short-range order than the calculated data shown in Fig. 1; hence the volumes of these samples must necessarily be smaller than the calculated data.

### D. Bulk modulus

It is the isothermal compressibility $\kappa_T$ that is directly obtained from isobaric-isothermal simulations using Eq. (8), but in order to enable comparisons with available experimental data, we compute the adiabatic bulk modulus $B_S$ through the thermodynamic relation: $1/B_S = 1/B_T - \alpha^2 VT/C_p$, where $B_T$ is the inverse of $\kappa_T$ or the isothermal bulk modulus. The calculated $B_S$ is shown in Fig. 5 as a function of temperature for the four gallium concentrations. For reference, the figure also includes the ultrasonic data for 3.3 at.% gallium of a single crystal at ambient temperature [42] and of a polycrystal at high temperatures [63]. It should be noted that the bulk modulus of the original MEAM potential in Ref. [36] adopted as the Pu1 state in the present model is fitted at 0 K to reproduce the room-temperature bulk modulus data for a dilute-gallium alloy [42].

The present model predicts growing stiffness with increasing gallium concentration, being consistent with the GGA predictions made in Ref. [64], as well as the trend of the liquidus curve on the Pu-Ga phase diagram. The relative increase in bulk modulus with respect to unalloyed $\delta$-Pu, 1.07, 1.20, and 1.31 for 2, 4, and 6 at.% gallium, respectively, all at 300 K, is close to the same data from the aforementioned GGA predictions, 1.04, 1.09, and 1.15, at 0 K. It is also comparable with the experimental data for the polycrystalline samples provided in Ref. [65], which indicate a 13% increase at 300 K for the gallium concentration around 6 at.%. We also note that the resonant ultrasound spectroscopy data for the gallium concentrations of 2.36–4.64 at.% measured near room temperature [64,66] lie more or less between the data for 2 and 4 at.% gallium obtained from the present model. The progressive increase of the bulk modulus upon gallium addition predicted from our model appears inconsistent with the irregular gallium concentration dependence reported in Ref. [64]. It should be noted, however, that at least the sample with 2.36 at.% gallium used in their measurements does not seem to have a single-phase $\delta$ structure around ambient temperature due to the weak stability of the $\delta$ phase at such a low gallium concentration at that temperature [66].

The model predicts the rate of thermal softening to be nearly independent of gallium concentration, which is also in accordance with experimental observations [63,64,66,67]. The observed gallium-concentration independence of the rate of thermal softening is somewhat nontrivial. It may seem that a system with a higher gallium concentration should generate weaker thermal softening, since the excess softening is induced

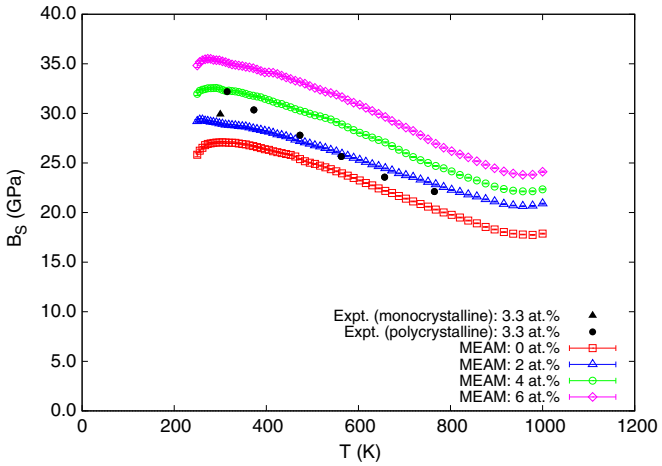


FIG. 5. (Color online) Calculated temperature dependence of the adiabatic bulk modulus for varying gallium concentration. The experimental data for monocrystalline [42] and for polycrystalline [63] 3.3 at.%–gallium alloys are also included for reference.

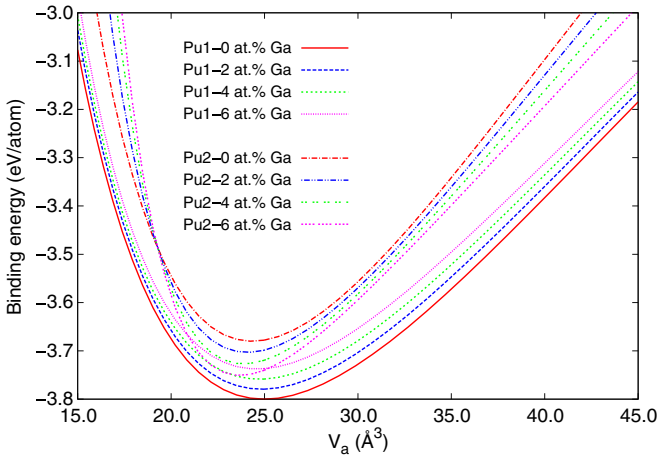


FIG. 6. (Color online) Binding energies of the Pu1-Ga and Pu2-Ga systems plotted as a function of atomic volume for varying gallium concentration.

by the thermal excitation between the two plutonium states. However, the slope of the bulk moduli was found to strike a subtle balance between the decrease in Invar entropy and the increase in the mixing entropy with respect to gallium addition. The calculated temperature slope of the bulk modulus, on the other hand, is less steep than the experimental data from the references quoted above, near or below ambient temperature. Essentially the same argument for the disagreement in low-temperature volume in the foregoing discussion would apply to the cause of the discrepancy in stiffness. The quenched $\delta$-phase samples below the eutectoid temperature should contain more Pu2 atoms, which form stiffer bonds with gallium atoms than Pu1 atoms do; thus the bulk moduli measured for these samples would be larger than the calculated data.

### E. Change in the energy-volume relationship with gallium concentration and its connection with thermodynamic properties

It is illuminating to reinterpret the simulation results described above in the light of the energy-volume relationship of the system. Shown in Fig. 6 is the variation of the binding energy curves of the Pu1 and Pu2 states with gallium concentration. In calculating these energies, the distribution of the gallium atoms is determined from the lowest-temperature configuration obtained from an MC simulation individually performed for the Pu1-Ga or Pu2-Ga system at each concentration. The volume of the periodic cell is isotropically varied while maintaining a perfect fcc lattice. The gallium distribution and relaxation effect were both found to have virtually no effect on the appearance of Fig. 6, however. The energy-volume relationship in pure $\delta$-Pu is indicative of the Invar behavior, where the energetically higher-lying Pu2 state is lower in volume in equilibrium than the Pu1 state. As gallium is added, the Pu1 state is elevated in energy while the Pu2 state is lowered, reflecting the difference between the Pu1-Ga and Pu2-Ga interactions. As a consequence, a reversal in the relative stability between the two plutonium states takes place at about 5 at.% gallium in the present model. Above this gallium concentration, the system displays an energy-volume relationship characteristic of anti-Invar systems, in which the Pu2 state is energetically lower than the Pu1 state in equilibrium. This transition from Invar to anti-Invar upon alloying is analogous to the iron-based Invar alloys [23,58,68,69]. (But in the opposite sense. For instance, introduction of nickel into $\gamma$-Fe promotes a transition from anti-Invar to Invar.) The above discussion is based on the binding energy per atom without taking into account the interactions between Pu1 and Pu2 atoms, but the actual relative composition between the Pu1 and Pu2 states and their distribution at a given gallium concentration are determined such that the total energy of the system is minimized. With the addition of gallium, which favors forming short and stiff bonds with Pu2 atoms, the system accommodates a greater number of the Pu2 atoms. Accordingly, the equilibrium volume of the total energy shifts toward a smaller value, and the bulk modulus becomes higher.

In understanding the characteristic temperature behavior of the system and its sensitivity to dilute-gallium alloying, it is useful to take a closer look at the fluctuation formulas, Eqs. (6)–(8), in view of the change of the energy-volume relationship with respect to gallium concentration shown in Fig. 6. Let us first see how strong thermal softening can be compatible with negative thermal expansion in the case of unalloyed $\delta$-Pu. $C_p$ and $\kappa_T$ are respectively expressed in terms of the variances of energy and volume, while $\alpha$ is related to the covariance of those variables. At low temperatures, for which the plutonium atoms predominantly occupy the Pu1 state, both of the deviations in energy and volume from their average values, $U - \langle U \rangle$ and $V - \langle V \rangle$, respectively, are negative, so that the three quantities, $C_p, \alpha$, and $\kappa_T$, are all positive, owing to the asymmetry of the binding-energy curve with respect to the equilibrium volume. The thermal softening is accompanied by positive thermal expansion in this case, as in ordinary metals. Recall now that, in unalloyed $\delta$-Pu, the Pu2 state lies higher in energy but lower in equilibrium volume than the Pu1 state, as shown in Fig. 6. At intermediate temperatures, the average volume can gradually shift toward a smaller value, as the Pu2

state becomes thermally populated. When a sufficient number of the plutonium atoms begin to occupy the Pu2 state, $V - \langle V \rangle$ can become increasingly positive. Consequently, $\alpha$ can be progressively driven to a negative value if the above volume contraction effect outweighs the usual volume expansion due to lattice anharmonicity. At the same time, $U - \langle U \rangle$ remains negative but its magnitude can grow significantly as a greater number of microstates becomes accessible to the system. Both $C_p$ and $\kappa_T$ experience a marked increase at elevated temperature, giving rise to the Schottky-like peak and the strong thermal softening, respectively. The Pu2 occupancy is saturated at higher temperatures for which the substantial lattice anharmonicity leads to an increase in the average volume, so that $\alpha$ recovers a positive value.

When the system is doped with a few at.% gallium (2–4 at.%), an appreciable fraction of the plutonium atoms is energetically promoted to the Pu2 state at low temperatures. In this case, the energies of the two plutonium states come closer to each other, as illustrated in Fig. 6. The fluctuation in the total energy, or $C_p$, accordingly becomes smaller than in the case of unalloyed $\delta$-Pu at the temperatures for which the thermal excitation between the two states takes place. (Yet the above effect can be overridden by the enhanced contribution from the mixing entropy, so that the overall heat capacity undergoes an increase with gallium addition, as discussed in Sec. III B.) Although the energy-volume relationship at these gallium concentrations indicates that the thermal excitation between the two states still acts to suppress the average volume, the positive expansion due to lattice anharmonicity begins to counteract the volume contraction effect with a significant weight by driving $V - \langle V \rangle$ from positive to negative (thus $\alpha$ from negative to positive). Upon further alloying (above 6 at.%), a considerable fraction of the plutonium atoms occupies the Pu2 state at low temperatures. The Pu2 state with a small equilibrium volume lies lower in energy than the Pu1 state in this case (Fig. 6). The thermal excitation between these two states now shifts $V - \langle V \rangle$ toward an increasingly negative value, which in turn enhances positive volume expansion in tandem with lattice anharmonicity.

### F. Local structure

We investigate the local atomic structure by computing partial radial-distribution functions for each type of elemental pair. Shown in Fig. 7 are the data for 4 at.% gallium calculated at 300 K and 700 K, as examples. These data display peaks at the positions whose ratios are characteristic of the fcc lattice at all temperatures examined in this study. The data obtained at 300 K are shown in Figs. 7(a) and 7(b) for the like and unlike pairs, respectively. These data indicate the presence of an $L1_2$-like short-range order in the domain composed of the Pu2 and gallium atoms (gallium-rich domain), which is segregated from the other domain of the Pu1 atoms (gallium-depleted domain). The Ga-Ga pair distribution shows a vanishingly low peak at the first-nearest neighbor distance and a relatively low peak at the third-nearest neighbor distance, along with an eminently high peak at the second- and fourth-nearest neighbor distances. In contrast, the Pu2-Ga pair distribution shows virtually no peak at the second- and fourth-nearest neighbor distances, while it shows a relatively high peak at the first-nearest neighbor distance and a rather high peak at the third-nearest neighbor distance. It should be noted that the profile of the first-nearest neighbor peak of the Pu2-Ga pair as well as that of the Pu1-Pu2 pair would be highly subject to the fraction of the interfaces of the two types of domains mentioned above. These domains are almost completely separated in the small periodic cell used in this study, but the actual morphology of these domains depends largely on the microstructure, which we can only address by the use of a sufficiently large periodic cell. The peaks of the Pu1-Ga pair distribution are rather low at short distances in the calculated data, but they are also dependent on the conformation of the two domains. Greater broadening of the peaks is generally observed at long distances, reflecting the appreciable departure from the perfect fcc lattice mainly due to the variation in the bond lengths associated with distinct elemental pairs. We found that a system with a higher gallium concentration exhibits greater lattice disorder in qualitative agreement with EXAFS observations [6,7].

The same data calculated at 700 K are shown in Figs. 7(c) and 7(d). The data peaks are in general wider and shallower than their counterparts at 300 K because of larger atomic vibrations. The position of each peak, however, shows little change from that at 300 K, particularly at short distances. The characteristics of the $L1_2$-like short-range order observed at low temperatures are much less pronounced, on account of a larger mixing entropy as well as a higher Pu2 occupancy at this temperature. The Ga-Ga pair distribution exhibits relatively high peaks at short distances, indicating that the gallium atoms are still fairly well clustering even at this temperature.

The Pu2-Ga bond length computed at 300 K is about 3.22 Å [for 4 at.% gallium; Fig. 7(b)], which is shorter than the Pu1-Pu1 bond by about 1.9%. The Pu2-Ga bond is larger than the Pu-Ga bond measured in EXAFS for similar dilute gallium concentrations, indicating contractions by 3%–4% [5,6,9]. The discordance can be attributed to the discrepancy in the atomic volumes below the eutectoid temperature, discussed in Sec. III C. Alternatively, it can be related to the fact that the Pu2-Ga bond length in the present model was fitted to the experimental Pu-Ga bond length in the $L1_2$ $Pu_3Ga$ compound at room temperature, 3.187 Å [4], as described in Sec. II B. It would be reasonable to envisage that the short-range order observed in our simulations at dilute gallium concentrations is connected to the $L1_2$ long-range order in the $Pu_3Ga$ reference alloy. Given that a system with a high gallium concentration has a propensity for anti-Invar behavior, it is expected that the reference alloy would have significantly large, positive thermal expansion. If the Pu2-Ga bond length had been fitted to the low-temperature EXAFS data of the Pu-Ga bond length in dilute alloys, it could have provided a superior description of the local structure of $\delta$ Pu-Ga alloys over a broader range of concentrations.

The calculated Pu2-Pu2 bond length is about 3.23 Å at 300 K [Fig. 7(a)]. This value also indicates inward contraction from its fitted value at 0 K, 3.253 Å, because of the tendency of the gallium atoms to form cuboctahedra with their twelve nearest-neighbor Pu2 atoms. Note that, at finite temperature, there are some Pu2 atoms not participating in the formation of the cuboctahedra but which are there merely because of thermal agitation, so that the average Pu2-Pu2 bond is

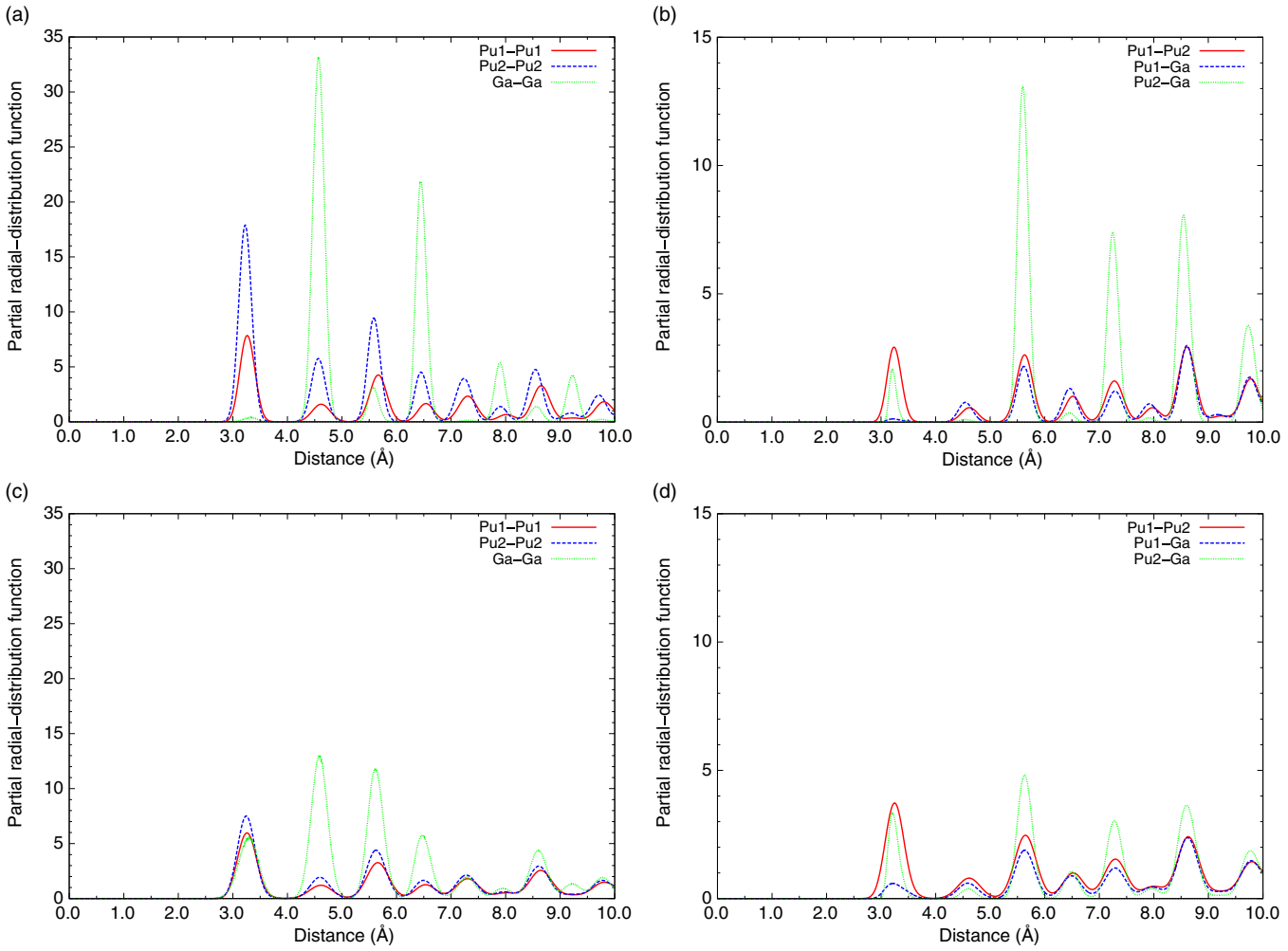


FIG. 7. (Color online) Calculated partial radial-distribution functions for 4 at.% gallium. (a) Like-pair distributions at 300 K. (b) Unlike-pair distributions at 300 K. (c) Like-pair distributions at 700 K. (d) Unlike-pair distributions at 700 K.

slightly longer than Pu2-Ga bonds at the same temperature. We indeed observed that the mismatch between the average Pu2-Ga and Pu2-Pu2 bond distances is more pronounced at higher temperatures. The Pu1-Pu1 bond length, about 3.27 Å at 300 K, also reduced from its fitted value at 0 K, 3.281 Å, induced by the overall volume contraction at the finite gallium concentration. All bonds are found to show inward contraction in the proximity of gallium atoms, but the effect is insignificant beyond first-nearest neighbor shells, where the contraction becomes less than 1%. The model predicts that, while the local structure is essentially independent of gallium concentration, each bond undergoes weak but progressive contraction with increasing gallium content, in qualitative agreement with a recent EXAFS study [8].

Experimentally, the gallium-replete domains are not found to be $L1_2$ $Pu_3Ga$ [11]. But one may observe that these experiments were conducted at the temperatures below the eutectoid point, below which the $\delta$ phase is not the lowest free-energy state. Thus the samples used in these measurements should be in some metastable states quenched from a certain high temperature, thus hindering detailed comparison with the above simulation results.

## IV. REMARKS AND DISCUSSION

The presence of the Invar effect in the $\delta$ phase seems to suggest an important implication for the stability mechanism of this phase, which is a matter of great interest in practice. Given the appreciable difference between the Debye temperatures of the $\alpha$ and $\delta$ phases [26], it is not clear whether or not the Invar effect plays a decisive role in the qualitative appearance of the $\delta$ phase at finite temperature. Yet, the Invar entropy in the $\delta$ phase, along with the mixing entropy, should contribute to the lowering of the free energy of this phase with respect to competing phases, and to have a nonnegligible influence on the occurrence of the eutectoid reaction at the relatively low temperature indicated on the phase diagram.

The entropy associated with the transformation from the $\delta$ to $\alpha'$ phases is found to be considerably large (1.3–1.4 $k_B$/atom [59,70–72]). The authors of Refs. [71,72] demonstrated that the vibrational contribution accounts for only about a quarter or less of the total transformation entropy, while the contributions for a major portion of the entropy remain unexplained. It was further pointed out that the Invar entropy estimated by means of the Weiss model for $\delta$-Pu of Ref. [20] would necessarily give rise to less than

0.1 $k_B$/atom [72]; hence it does not account for the large entropy. This indeed turns out to be the case for the present interacting atomistic model, which is likely because this particular parametrization for the cross-interaction between Pu1 and Pu2 was developed to be qualitatively similar to the noninteracting Weiss model of Ref. [20], as described in Sec. II B. However, a different choice of interaction parameters or the inclusion of additional participating states (which may involve large magnetic moments) could conceivably generate an entropic contribution much larger than that obtained from the present model.

The analysis given in this study is based on the use of a relatively small periodic cell, and is focused on the local atomic environment within the bulk fcc structure. Although some types of the trial moves (such as exchanges between the positions of different elements as well as parallel tempering) exploited in the present MC simulations are convenient to circumvent the sampling difficulty attendant on high interface free energies, the use of such a small supercell does not accommodate long-range relaxations, and is incapable of addressing the microstructural aspects relevant to phase transformations. Detailed analysis of relative phase stability by way of an atomistic model requires simulations with a sufficiently large periodic cell, in addition to explicit free energy computations [16,17,37,73]. Investigation of these issues goes beyond the scope of this paper and is left to future work.

The relationship between the present two-state model and an electronic-level understanding is unclear, in part due to the ongoing attempts to provide a consistent electronic-structure description of this system. One possible interpretation is to think of the two binding-energy curves in the present model as the total energies of the $5f^6$ and $5f^5$ configurations. Correspondingly, we interpret the plutonium atoms in the Pu1 and Pu2 states, respectively, as $Pu^{2+}$ and $Pu^{3+}$ ions, being distinct species. The relative stability between these configurations may be sensitive to dilute alloying with gallium, as discussed in Sec. III E. In the dynamical mean-field theory picture, the ground state of $\delta$-Pu dynamically fluctuates between these two configurations, leading to Kondo screening of the magnetic moment, up to a characteristic temperature of the order of 800 K [74]. This mixed-valance nature has recently been supported by resonant x-ray emission spectroscopy and x-ray absorption near-edge structure spectroscopy experiments [75]. The relative time the electron spends in one of these configurations determines the intermediate valence, resulting in a noninteger value for the average $f$-electron occupancy ($\sim$5.2–5.3) [76]. In the classical description suggested in the present study, in contrast, the transition between these two atomic-valence states is thermally induced according to the Schottky statistics. Clearly, such a classical view in terms of the static valence states is not equivalent to the aforementioned quantum-mechanical description. Note, however, that if the valence fluctuation reaches a high-temperature regime, then it would couple to the vibrational modes, thereby giving rise to nontrivial thermal properties including anomalous thermal expansion. Such an effect has been observed in some rare-earth compounds [77,78]. It would not be absolutely unreasonable to envision that the long-time average properties obtained from an effective classical model describing the dynamics of the valence fluctuations would be addressed by the equilibrium properties obtained from a stochastic classical model, presumably with the Schottky statistics, at least at high temperatures.

Another interpretation would be to view the binding-energy curve for the Pu1 state as an effective representation of the energy-volume relationship of the electronic ground state of $\delta$-Pu, perhaps characterized in its entirety by a mixed valence. Then the binding curve for the Pu2 state defines the energy-volume relationship of an electronic excited state, most likely with a valence or magnetic state distinct from that of the ground state. The energy separation between those states that is comparable with the thermal energy may be associated with some combination of the effective band-splitting that occurs due to spin-orbit coupling and the crystal field. In this case, and as before, we may envisage that the high-temperature equilibrium properties of the system can be well approximated by the classical model proposed in this study.

## V. CONCLUSIONS

We have developed an atomistic model that captures a range of anomalous features of the $\delta$ phase of the Pu-Ga alloys in a coherent manner. The model is structured on the following two fundamental mechanisms:

(1) The plutonium atoms in the fcc structure are characterized by two distinct electronic states, Pu1 and Pu2. The Pu2 state lies higher in energy but lower in volume in equilibrium than the Pu1 state. The energy separation between these two states is comparable with the thermal energy, such that they are thermally accessible to one another.

(2) The plutonium atoms in the Pu2 state form energetically more stable, shorter, and stiffer bonds with gallium than those in the Pu1 state do.

The first mechanism ensures that unalloyed $\delta$-Pu is an Invar system. Addition of gallium impurities leads to a reversal in the relative stability between the Pu1 and Pu2 states at a dilute concentration on account of the second mechanism, so that the system undergoes a transition toward anti-Invar behavior.

In summary, the model accounts for the following experimental observations:

(a) Negative thermal expansion and strong thermal softening in unalloyed $\delta$-Pu are naturally reconciled. Owing to the first mechanism, the average volume becomes suppressed as a growing fraction of the small Pu2 state becomes populated with increasing temperature. Negative thermal expansion takes place when this volume contraction effect outweighs the usual lattice anharmonicity. The same effect of volume contraction concomitantly gives rise to pronounced thermal softening, which would have been incompatible with negative thermal expansion if the Invar mechanism were absent.

(b) The model provides a consistent description of both excessive volume reduction and a rapid change in thermal expansion upon dilute-gallium alloying. Presence of gallium impurities induces substantial gains at low temperatures in the number of Pu2 atoms, which form short bonds with the gallium atoms according to the second mechanism. The same mechanism results in an overall depletion of Pu1 atoms, which in turn suppresses the thermal contraction effect due to the

presence of two plutonium states in the first mechanism. The thermal-expansion coefficient thereby shifts toward a positive value as gallium concentration is raised. The reproduction of the temperature dependence of the atomic volume is excellent for all the gallium concentrations examined in this study.

(c) The predicted bulk modulus exhibits progressive overall stiffening with increasing gallium concentration, in accordance with a recent GGA prediction. This effect is linked to the growing number of stiff Pu2-Pu2 and Pu2-Ga bonds with increasing gallium concentration as a consequence of the second mechanism. The calculated temperature variation of the bulk modulus is, in contrast, nearly concentration independent as observed in resonant ultrasound spectroscopy experiments. This independence is the outcome of a subtle balance between the diminished contribution from the Invar effect and the enhanced contribution from interdiffusion with respect to gallium concentration.

(d) The model offers a cogent explanation for the nanoscale heterogeneity observed in dilute-gallium alloys from EXAFS experiments. Gallium impurity atoms exhibit a propensity to form cuboctahedra with their twelve Pu2 neighbors by virtue of the second mechanism, inducing inward contraction in their vicinity. At sufficiently low temperatures, these cuboctahedra cluster together to form gallium-rich domains with short-range order, which are segregated from gallium-depleted domains comprised of Pu1 atoms. The gallium atoms increasingly spread over wider regions of the system at elevated temperature, as Pu2 atoms are thermally populated due to the first mechanism. As a result, the fcc lattice is increasingly disordered with growing gallium concentration. The distribution of these gallium atoms does not become completely random because of the short-range order persisting up to high temperatures, resulting in nanoscale heterogeneity, as would be observed for quenched samples. Apart from minor but progressive contraction in each bond length with increasing gallium concentration, the local structure remains largely uninfluenced by the concentration.

Note that it is only the foregoing two mechanisms that govern this variety of characteristic macroscopic properties. The ostensible incompatibility among properties in the conventional single-state atomistic description has been resolved in a clear-cut way, and the diverse phenomenologies have been integrated into a comprehensive view in terms of the two-state model.

While the idea behind this study is inspired by the earlier work based on the noninteracting Weiss model [19,20], the quantitative introduction of effective atomic interactions in the present atomistic model adds significant value in providing a more detailed microscopic description of the system. It should be noted, in particular, that the dilute-alloying mechanism hypothesized in Ref. [20] can only be built into an interacting model, as in the second mechanism above. In principle, the MC approach employed in this study enables us to calculate the entropy for a given interatomic-potential model in an exact manner. The major strength of the approach lies in its capability of making a direct connection between the local atomic structure and the full equation of state of a solid, including its sensitivity to shear deformations. (An analysis of shear elastic constants would require a more extensive fitting database for interatomic potentials than used in this study, however.) Such an approach is essential for a description of crystalline defects, which is one of the key issues concerning radiation damage effects and long-term stability [34,38–40,79–84]. The present atomistic scheme offers an analytical basis for investigating the influence of the Invar effect on the equilibrium properties of $\delta$ Pu-Ga alloys that include, for example, point defects or interfaces. At the same time, the implementation of the two-state model into molecular dynamics is a separate, nontrivial question, which will most likely involve a nonadiabatic treatment [85–87].

Owing to the scarcity of experimental inputs as well as the lack of certainty in modern first-principles calculations for this system, the present model retains a fair degree of empiricism, particularly in the characterization of fine details of the interatomic potentials. To provide a more satisfactory description, the free parameters in the interatomic potentials would have to be determined on the basis of accurate electronic-structure calculations. As noted earlier, the two-state description in the present atomistic model is a simple phenomenology based on an analogy to the Weiss model, and it does not address the electronic origin of the two states or the underlying physics of the transition mechanism between them. It is possible that $\delta$-Pu encompasses a variety of complex electronic configurations within a narrow energy range, and that the conception in terms of only two electronic states turns out to be an oversimplification. Nevertheless, the present model provides highly consistent, although unconventional, explanations at the atomic scale for multiple macroscopic anomalies with respect to temperature and dilute alloying that were previously deemed intractable. This success is rather remarkable, particularly in view of the fact that the mechanisms underlying the model energetics are strikingly simple ones. Whether or not the quantitative descriptions given in this study are correct in all details, it seems that the general picture we have put forward would remain unaltered. The challenge we now wish to be addressed is whether we can find any specific evidence, either theoretical or experimental, for or against the actual validity of the Invar description of $\delta$-Pu and its alloys.

## ACKNOWLEDGMENTS

The authors are grateful to Jim Doll, Jim Gubernatis, Albert Migliori, Babak Sadigh, Paul Tobash, Ilya Vekhter, Art Voter, and Jianxin Zhu for useful discussions. This work is performed through the LANL LDRD program under the auspices of Los Alamos National Security, LLC, for the National Nuclear Security Administration of the US DOE under Contract No. DE-AC52-06NA25396. S.P.C. acknowledges the support of the LANL ASC program. S.D.C. acknowledges the support of the Division of Chemical Sciences, Geosciences, and Biosciences, Office of Basic Energy Sciences, US DOE, under the Heavy Element Chemistry Program at LANL.

[1] S. S. Hecker, in *Challenges in Plutonium Science*, Los Alamos Science, edited by N. G. Cooper, Vol. 26 (Los Alamos National Laboratory, Los Alamos, NM, 2000), pp. 290–335.

[2] S. S. Hecker, D. R. Harbur, and T. G. Zocco, Prog. Mater. Sci. **49**, 429 (2004).

[3] G. D. Barrera, J. A. O. Bruno, T. H. K. Barron, and N. L. Allan, J. Phys.: Condens. Matter **17**, R217 (2005).

[4] F. H. Ellinger, C. C. Land, and V. O. Struebing, J. Nucl. Mater. **12**, 226 (1964).

[5] L. E. Cox, R. Martinez, J. H. Nickel, S. D. Conradson, and P. G. Allen, Phys. Rev. B **51**, 751 (1995).

[6] P. Faure, B. Deslandes, D. Bazin, C. Tailland, R. Doukhan, J. M. Fournier, and A. Falanga, J. Alloys Compd. **244**, 131 (1996).

[7] S. D. Conradson, in *Challenges in Plutonium Science*, Los Alamos Science, edited by N. G. Cooper, Vol. 26 (Los Alamos National Laboratory, Los Alamos, NM, 2000), pp. 356–363.

[8] C. H. Booth, Y. Jiang, S. A. Medling, D. L. Wang, A. L. Costello, D. S. Schwartz, J. N. Mitchell, P. H. Tobash, E. D. Bauer, S. K. McCall, M. A. Wall, and P. G. Allen, J. Appl. Phys. **113**, 093502 (2013).

[9] P. G. Allen, A. L. Henderson, E. R. Sylwester, P. E. A. Turchi, T. H. Shen, G. F. Gallegos, and C. H. Booth, Phys. Rev. B **65**, 214107 (2002).

[10] E. J. Nelson, K. J. M. Blobaum, M. A. Wall, P. G. Allen, A. J. Schwartz, and C. H. Booth, Phys. Rev. B **67**, 224206 (2003).

[11] S. D. Conradson *et al.*, J. Phys. Chem. C **118**, 8541 (2014); S. D. Conradson [Phys. Rev. B (to be published)].

[12] J. D. Becker, J. M. Wills, L. Cox, and B. R. Cooper, Phys. Rev. B **58**, 5143 (1998).

[13] B. Sadigh and W. G. Wolfer, Phys. Rev. B **72**, 205122 (2005).

[14] K. T. Moore, P. Söderlind, A. J. Schwartz, and D. E. Laughlin, Phys. Rev. Lett. **96**, 206402 (2006).

[15] K. T. Moore, D. E. Laughlin, P. Söderlind, and A. J. Schwartz, Philos. Mag. **87**, 2571 (2007).

[16] G. Robert, C. Colinet, B. Siberchicot, and A. Pasturel, Modelling Simul. Mater. Sci. Eng. **12**, 693 (2004).

[17] G. Robert, C. Colinet, B. Siberchicot, and A. Pasturel, Philos. Mag. **84**, 1877 (2004).

[18] O. Eriksson, J. N. Becker, A. V. Balatsky, and J. M. Wills, J. Alloys Compd. **287**, 1 (1999).

[19] A. C. Lawson, J. A. Roberts, B. Martinez, and J. W. Richardson, Jr., Philos. Mag. **82**, 1837 (2002).

[20] A. C. Lawson, J. A. Roberts, B. Martinez, M. Ramos, G. Kotliar, F. W. Trouw, M. R. Fitzsimmons, M. P. Hehlen, J. C. Lashley, H. Ledbetter, R. J. McQueeney, and A. Migliori, Philos. Mag. **86**, 2713 (2006).

[21] R. J. Weiss, Proc. Phys. Soc. **82**, 281 (1963).

[22] T. Lee, M. I. Baskes, A. C. Lawson, S. P. Chen, and S. M. Valone, Materials **5**, 1040 (2012).

[23] M. E. Gruner, R. Meyer, and P. Entel, Eur. Phys. J. B **2**, 107 (1998).

[24] T. Yokoyama and K. Eguchi, Phys. Rev. Lett. **107**, 065901 (2011).

[25] T. Yokoyama and K. Eguchi, Phys. Rev. Lett. **110**, 075901 (2013).

[26] A. C. Lawson, J. A. Goldstone, B. Cort, R. J. Martinez, F. A. Vigil, T. G. Zocco, J. W. Richardson, and M. H. Mueller, Acta Cryst. B **52**, 32 (1996).

[27] D. A. Kofke and E. D. Glandt, Mol. Phys. **64**, 1105 (1988).

[28] D. Frenkel and B. Smit, *Understanding Molecular Simulation: From Algorithms to Applications*, 2nd ed. (Academic Press, San Diego, 2002).

[29] W. W. Wood, J. Chem. Phys. **48**, 415 (1968).

[30] C. J. Geyer, in *Computing Science and Statistics: Proceedings of the 23rd Symposium on the Interface*, edited by by E. M. Keramidas (Interface Found. Amer., Fairfax Station, VA, 1991), pp. 156–163.

[31] K. Hukushima and K. Nemoto, J. Phys. Soc. Jpn. **65**, 1604 (1996).

[32] M. P. Allen and D. J. Tildesley, *Computer Simulation of Liquids* (Oxford University Press, New York, 1987).

[33] P. Söderlind, G. Kotliar, K. Haule, P. M. Oppeneer, and D. Guillaumont, MRS Bulletin **35**, 883 (2010).

[34] V. I. Anisimov, V. V. Dremov, M. A. Korotin, G. N. Rykovanov, and V. V. Ustinov, Phys. Metals Metallogr. **114**, 1087 (2013).

[35] M. I. Baskes, Phys. Rev. B **46**, 2727 (1992).

[36] M. I. Baskes, Phys. Rev. B **62**, 15532 (2000).

[37] M. I. Baskes, K. Muralidharan, M. Stan, S. M. Valone, and F. J. Cherne, JOM **55**, 41 (2003).

[38] M. I. Baskes, A. C. Lawson, and S. M. Valone, Phys. Rev. B **72**, 014129 (2005).

[39] S. M. Valone, M. I. Baskes, and R. L. Martin, Phys. Rev. B **73**, 214209 (2006).

[40] M. I. Baskes, S. Y. Hu, S. M. Valone, G. F. Wang, and A. C. Lawson, J. Computer-Aided Mater. Des. **14**, 379 (2007).

[41] B. J. Thijsse, Nucl. Instrum. Methods Phys. Res., Sect. B **228**, 198 (2005).

[42] H. M. Ledbetter and R. L. Moment, Acta Metall. **24**, 891 (1976).

[43] S. P. Chen, Philos. Mag. **89**, 1813 (2009).

[44] S. S. Hecker and L. F. Timofeeva, in *Challenges in Plutonium Science*, Los Alamos Science, edited by N. G. Cooper, Vol. 26 (Los Alamos National Laboratory, Los Alamos, NM, 2000), pp. 244–251.

[45] S. Strässler and C. Kittel, Phys. Rev. **139**, A758 (1965).

[46] M. I. Baskes, S. P. Chen, and F. J. Cherne, Phys. Rev. B **66**, 104107 (2002).

[47] A. Landa, P. Söderlind, and A. Ruban, in *Plutonium Futures—the Science*, edited by G. D. Jarvinen, AIP Conf. Proc., Vol. 673 (AIP, Melville, NY, 2003), pp. 159–161.

[48] M. I. Baskes, Mater. Chem. Phys. **50**, 152 (1997).

[49] C. Predescu, M. Predescu, and C. V. Ciobanu, J. Chem. Phys. **120**, 4119 (2004).

[50] T. Lee, M. I. Baskes, S. M. Valone, and J. D. Doll, J. Phys.: Condens. Matter **24**, 225404 (2012).

[51] D. Sabo, C. Predescu, J. D. Doll, and D. L. Freeman, J. Chem. Phys. **121**, 856 (2004).

[52] A. Srinivasan, D. M. Ceperley, and M. Mascagni, Adv. Chem. Phys. **105**, 13 (1999).

[53] F. L. Oetting and R. O. Adams, J. Chem. Thermodyn. **15**, 537 (1983).

[54] R. O. Adams and F. L. Oetting, J. Nucl. Mater. **118**, 269 (1983).

[55] A. E. Kay and R. G. Loasby, Philos. Mag. **9**, 37 (1964).

[56] R. L. Rose, J. L. Robbins, and T. B. Massalski, J. Nucl. Mater. **36**, 99 (1970).

[57] R. L. Rose, J. L. Robbins, and T. B. Massalski, J. Nucl. Mater. **75**, 98 (1978).

[58] W. Pepperhoff and M. Acet, *Constitution of Magnetism of Iron and its Alloys* (Springer, Heidelberg, 2001).

[59] J. C. Lashley, J. Singleton, A. Migliori, J. B. Betts, R. A. Fisher, J. L. Smith, and R. J. McQueeney, Phys. Rev. Lett. **91**, 205901 (2003).
[60] A. C. Lawson and J. C. Lashley, Philos. Mag. **93**, 2377 (2013).
[61] A caveat is warranted concerning the gallium concentrations of the samples used in the neutron diffraction experiments of Ref. [19]. A recalibration of the gallium concentrations based on the actual values of their lattice constants appears to indicate that the samples marked as 2, 4, and 6 at.% would more probably have concentrations of 1.91, 3.01, and 5.37 at.%, respectively [88].
[62] J. M. Taylor, J. Nucl. Mater. **31**, 339 (1969).
[63] C. A. Calder, E. C. Draney, and W. W. Wilcox, J. Nucl. Mater. **97**, 126 (1981).
[64] P. Söderlind, A. Landa, J. E. Klepeis, Y. Suzuki, and A. Migliori, Phys. Rev. B **81**, 224110 (2010).
[65] J. C. Taylor, P. F. T. Linford, and D. J. Dean, J. Inst. Metals **96**, 178 (1968).
[66] A. Migliori, H. Ledbetter, A. C. Lawson, A. P. Ramirez, D. A. Miller, J. B. Betts, M. Ramos, and J. C. Lashley, Phys. Rev. B **73**, 052101 (2006).
[67] A. Migliori, F. Freibert, J. C. Lashley, A. C. Lawson, J. P. Baiardo, and D. A. Miller, J. Superconductivity **15**, 499 (2002).
[68] V. L. Moruzzi, P. M. Marcus, and J. Kübler, Phys. Rev. B **39**, 6957 (1989).
[69] E. F. Wassermann and P. Entel, J. Phys. IV France **05**, C8 (1995).
[70] P. E. A. Turchi, L. Kaufman, S. Zhou, and Z.-K. Liu, J. Alloys Compd. **444–445**, 28 (2007).
[71] M. E. Manley, A. H. Said, M. J. Fluss, M. Wall, J. C. Lashley, A. Alatas, K. T. Moore, and Y. Shvyd'ko, Phys. Rev. B **79**, 052301 (2009).
[72] J. R. Jeffries, M. E. Manley, M. A. Wall, K. J. M. Blobaum, and A. J. Schwartz, Phys. Rev. B **85**, 224104 (2012).
[73] J. N. Mitchell, D. S. Schwartz, M. Stan, and C. J. Boehlert, Metall. Mater. Trans. A **35**, 2267 (2004).
[74] J. H. Shim, K. Haule, and G. Kotliar, Nature (London) **446**, 513 (2007).
[75] C. H. Booth, Y. Jiang, D. L. Wang, J. N. Mitchell, P. H. Tobash, E. D. Bauer, M. A. Wall, P. G. Allen, D. Sokaras, D. Nordlund, T.-C. Weng, M. A. Torrez, and J. L. Sarrao, Proc. Natl. Acad. Sci. USA **109**, 10205 (2012).
[76] It should be remarked that there have been both theoretical and experimental observations that there is likely at least one additional valence configuration ($5f^4$) that plays a role in plutonium [74,75,89,90].
[77] A. Jayaraman, P. Dernier, and L. D. Longinotti, Phys. Rev. B **11**, 2783 (1975).
[78] Y. Hiranaka *et al.*, J. Phys. Soc. Jpn. **82**, 083708 (2013).
[79] P. Pochet, Nucl. Instrum. Methods Phys. Res., Sect. B **202**, 82 (2003).
[80] B. P. Uberuaga, S. M. Valone, and M. I. Baskes, J. Alloys Compd. **444–445**, 314 (2007).
[81] S. M. Valone and M. I. Baskes, J. Computer-Aided Mater. Des. **14**, 357 (2007).
[82] A. Kubota, W. G. Wolfer, S. M. Valone, and M. I. Baskes, J. Computer-Aided Mater. Des. **14**, 367 (2007).
[83] L. Berlu, G. Jomard, G. Rosa, and P. Faure, J. Nucl. Mater. **374**, 344 (2008).
[84] M. Robinson, S. Kenny, R. Smith, M. Storr, and E. McGee, Nucl. Instrum. Methods Phys. Res., Sect. B **267**, 2967 (2009).
[85] J. C. Tully, Faraday Discuss. **110**, 407 (1998).
[86] C. P. Race, D. R. Mason, M. W. Finnis, W. M. C. Foulkes, A. P. Horsfield, and A. P. Sutton, Rep. Prog. Phys. **73**, 116501 (2010).
[87] A. A. Correa, J. Kohanoff, E. Artacho, D. Sánchez-Portal, and A. Caro, Phys. Rev. Lett. **108**, 213201 (2012).
[88] A. C. Lawson, Philos. Mag., doi:10.1080/14786435.2014.906759 (2014).
[89] E. S. Clementyev and A. V. Mirmelstein, J. Exp. Theor. Phys. **109**, 128 (2009).
[90] G. van der Laan and M. Taguchi, Phys. Rev. B **82**, 045114 (2010).